

A non-singular universe out of Hayward black hole

Michał Bobula^{a,b*}

^a*University of Wrocław, Faculty of Physics and Astronomy,*

Institute of Theoretical Physics, pl. M. Borna 9, 50-204 Wrocław, Poland and

^b*Instituto de Estructura de la Materia, IEM-CSIC, Serrano 121, 28006 Madrid, Spain*

We construct a (quantum mechanically) modified model for the Oppenheimer-Snyder collapse scenario where the exterior of the collapsing dust ball is a Hayward black hole spacetime and the interior is a dust Friedmann-Robertson-Walker cosmology. This interior cosmology is entirely determined by the junction conditions with the exterior black hole. It turns out to be non-singular, displaying a power-law contraction which precedes a de Sitter phase or, reversely, a power-law expansion followed by a de Sitter era. We also analyse the global causal structure and the viability of the model.

I. INTRODUCTION

The question of whether the spacetime singularities inherent to General Relativity (GR) represent a real physical phenomenon remains open more than a century after the advent of this gravitational theory. In cosmological scenarios, the debate affects fundamental questions about the origin of the Universe. Was there something before the Big Bang? Did the Universe have a beginning? In black hole physics, the problem is related to other important physical issues. What is the fate of free-falling observers? What happens beyond the event horizon? The classical Oppenheimer-Snyder (OS) collapse scenario [1] is a especially suitable arena to discuss the connection between the aforementioned questions. The fact that we can model a collapsing dust ball using a Friedmann-Robertson-Walker (FRW) metric in its interior and a Schwarzschild solution in the exterior suggests a link between black hole spacetimes and cosmology. Nevertheless, the resulting geometry still possesses a singularity, posing serious difficulties at the classical level and, more importantly, sustaining the black hole information paradox in a semiclassical picture of the black hole evaporation [2].

The singular nature of the Schwarzschild spacetime has motivated considerable effort devoted to exploring alternatives [3–38]. A prominent example is the Hayward black hole [5], on which we will focus our attention in this work. Instead of the singularity at the origin of the radial coordinate, this spacetime displays a regular ‘quantum gravity core’. The Hayward geometry has a really special conformal diagram, representing an evaporating non-singular black hole (in which back-reaction is effectively introduced) [5]¹. All matter entering the black hole ultimately reaches future null infinity. Hence, in a semiclassical approximation, most probably there is

enough Cauchy data at this future infinity to reconstruct the past, resolving the information paradox.

Although the Hayward metric seems to solve some fundamental problems present in the Schwarzschild metric, there has been no consensus about which physical theory the metric could be derived from. However, recently the metric has been derived as a vacuum solution within two independent effective descriptions incorporating quantum gravity corrections [29, 39]. The first one, called Quasi-Topological Theory [39, 40], can be regarded as Einstein-Hilbert action supplemented with an infinite tower of higher-curvature corrections which are contractions of the Riemann tensor. For instance, when the tower is truncated at the second order, one gets Gauss-Bonnet gravity (see Refs. [41, 42]). In general, such an infinite tower of corrections, weighted by powers of e.g. the Planck length, is what one could expect from String Theory (ST) as an ultraviolet completion of GR [42]. Specifically, when the number of spacetime dimensions D is equal or greater than five and spherical symmetry is imposed, the equations of motions (being of second differential order) determine the Hayward metric as a unique vacuum solution, provided that the simplest sequence of gravitational couplings is chosen [39]. The other aforementioned description [29], built in four spacetime dimensions, leads to the Hayward metric as the vacuum solution coming from a deformed (or “polymerized”) gravitational Hamiltonian in Lemaître-Tolman-Bondi (LTB) spacetimes. Motivated by dust collapse models in Loop Quantum Gravity (LQG), where the effective dynamics can be regarded as an LTB model with a polymerized Hamiltonian [27–29], the authors of Ref. [29] construct a specific “polymerization function” for the Hamiltonian that reproduces the Hayward metric in vacuo. Contrary to what happens in standard effective LQG models, the polymerization function is now unbounded. Moreover, this description can be translated into a Lagrangian mimetic gravity theory with a concrete mimetic potential.

In the present work, we will assume that the Hayward metric describes the vacuum exterior of a modified OS collapse scenario. We will then impose con-

* michal.bobula@uwr.edu.pl

¹ Although the associated static metric was originally derived by Poisson & Israel from the model inspired by one-loop corrections to Einstein field equations [3], its relevance for the information puzzle was established in Ref. [5].

ditions for the interior compatible with the above descriptions and derive the corresponding cosmological behavior. Indeed, we will explore the resulting interior dust cosmology when we require: a) both the exterior and interior metrics join smoothly at the boundary, located at the surface of the collapsing dust ball, b) a conservation law for dust is satisfied. This investigation should open the door to exploring how well the interior FRW background describes our universe.

The interior geometry will be completely determined just by imposing Israel-Darmois junction conditions at the boundary. The mathematical implementation of this condition and the formalism on which it is based were already studied by Pawłowski and the author in Refs. [23, 24], in the context of some effective models of OS collapse in LQG. In those previous works, it was the exterior metric that was determined in terms of the bouncing cosmology. More recently, similar techniques were also applied by several other authors [25, 27–29, 36, 43, 44]. The dust cosmology that we will obtain has the following remarkable features. It has no curvature singularities, it presents a de Sitter era preceding (following) a power-law expansion (contraction), and the transition between these two regimes is smooth, displaying a graceful exit. Moreover, we will see that our modified OS model shares the behavior found in Ref. [44] for a model inspired by Asymptotically Safe Gravity (ASG). Finally, we will also construct and discuss the conformal diagram representing the modified OS collapse (without back-reaction due to Hawking radiation).

II. COSMOLOGICAL DYNAMICS FROM JUNCTION CONDITIONS

We consider a modified OS collapse scenario, where the static exterior of the collapsing dust ball is given by the line element

$$ds_{\text{ext}}^2 = -F(X)dt^2 + \frac{1}{F(X)}dX^2 + X^2d\Omega^2, \quad (1)$$

where $d\Omega^2 = d\theta^2 + \sin^2\theta d\varphi^2$ is the metric on the two-sphere, and the function $F(X)$ is chosen to correspond to a Hayward black hole [5], namely

$$F(X) = 1 - \frac{2MX^2}{X^3 + 2l^2M}. \quad (2)$$

Here, M is a ‘mass’ constant. For large values of the radial coordinate X the metric behaves like the Schwarzschild one. The other constant in Eq. (2) is usually taken to be the Planck length (and hence $l = 1$ in the Planck units that we are adopting), although we will maintain it explicitly in our formulae. For small X , we have $F(X) \sim 1 - X^2/l^2$. Thus, we can expect that the cosmological interior that matches

smoothly at the boundary displays an epoch of de Sitter behavior. Throughout the rest of this article, we restrict the analysis to the non-extreme case when $M > (3\sqrt{3}/4)l$ in Eq. (2), so that the mass ranges over values of astrophysical interest. In this case, $F(X)$ has two positive roots, say $0 < X^- < X^+$.

For the homogeneous interior of the dust ball, on the other hand, we assume a flat FRW line element

$$ds_{\text{int}}^2 = -dT^2 + a(T)^2 dr^2 + r^2 a(T)^2 d\Omega^2. \quad (3)$$

The form of the scale factor $a(T)$ is determined by our junction conditions with the exterior. In full detail, we demand that the Israel-Darmois junction conditions (see e.g. Chapters 3.7-3.8 of Ref. [45]) be satisfied at the surface of the collapsing dust ball. We call Σ this boundary. Thus, the induced metric on Σ and its extrinsic curvature (second fundamental form) must coincide when computed from the exterior and from the interior, namely, $h_{ab}^{\text{ext}} = h_{ab}^{\text{int}}$ and $K_{ab}^{\text{ext}} = K_{ab}^{\text{int}}$, respectively. A detailed analysis of these conditions on the line elements (1) and (3) was recently carried out in Refs. [24, 25, 46]². Here, we will summarize the most important aspects. Let T be a parameter at Σ . The trajectory of the free-falling observer at Σ can be described either as $x_{\text{ext}}^\alpha = (t = \tau(T), X = R(T))$ from the exterior or as $x_{\text{int}}^\alpha = (T, r = r_b)$ from the interior, where r_b is a constant. The junction conditions form a soluble system of algebraic equations. They imply the following relations [24, 25, 46], that are crucial for this work:

$$X \Big|_{\Sigma} = R(T) = r_b a(T), \quad (4)$$

and

$$F \Big|_{\Sigma} = 1 - \dot{R}(T)^2, \quad (5)$$

where the dot denotes the derivative with respect to T . Note that T is the affine parameter for observers co-moving with the surface. In order to arrive at the above two equations, no particular form of $a(T)$ or $F(X)$ was assumed.

We can combine Eqs. (2), (4), and (5) to get

$$1 - \frac{2MR(T)^2}{R(T)^3 + 2l^2M} = 1 - \dot{R}(T)^2. \quad (6)$$

Integrating the negative root of $\dot{R}(T)$ (so that matter is contracting) with the initial condition $R(0) =$

² See Ref. [46] for the general analysis of the case where the exterior line element (1) is not necessarily stationary.

$R_0 = r_b a_0$, we obtain

$$T(a) = \frac{1}{3} \sqrt{\frac{2a_0^3 r_b^3}{M} + 4l^2} - \frac{1}{3} \sqrt{\frac{2a^3 r_b^3}{M} + 4l^2} - \frac{1}{3} l \log \left(\frac{\left(\sqrt{\frac{2a_0^3 r_b^3}{M} + 4l^2} + 2l \right) \left(\sqrt{\frac{2a^3 r_b^3}{M} + 4l^2} - 2l \right)}{\left(\sqrt{\frac{2a_0^3 r_b^3}{M} + 4l^2} - 2l \right) \left(\sqrt{\frac{2a^3 r_b^3}{M} + 4l^2} + 2l \right)} \right) \quad (7)$$

It is challenging to invert this equation to get $a(T)$. However, we can analyse it to deduce important properties of the resulting scale factor. One has $\lim_{a \rightarrow \infty} T(a) = -\infty$ and $\lim_{a \rightarrow 0} T(a) = \infty$. These limits, together with the fact that relation (7) is monotonic in $a \in (0, \infty)$, indicate that the inverse function $a(T)$ describes a timelike geodesically complete dust universe, in which matter is contracting for all values of the affine parameter $T \in (-\infty, \infty)$. Thanks to homogeneity, the scale factor obtained by solving the junction conditions is valid not only at Σ , but in the whole interior. Note that the log term dominates in Eq. (7) for small a , implying that the contraction of the Universe is exponential in this regime. On the other hand, for large a , the log contribution becomes negligible and the scale factor approximately behaves as for dust collapse in GR, namely, $a(T) \sim T^{2/3}$. Since the dependence of $T(a)$ given in Eq. (7) is smooth and strictly monotonic for $a \in (0, \infty)$, the deduced interior geometry admits a graceful exit from the de Sitter epoch. It is worth remarking that the Krestchmann scalar K_{int} is bounded everywhere in the interior (see Appendix A). In particular, in the limit $a \rightarrow 0$, when the metric (3) becomes degenerate, we have $K_{\text{int}} \rightarrow 24/l^4$.

If we write the energy density of the modified model of OS collapse as

$$\rho = \frac{3M}{4\pi r_b^3 a^3}, \quad (8)$$

a simple calculation leads us to the (quantum mechanically) modified Friedmann equations

$$\left(\frac{\dot{a}}{a} \right)^2 = \frac{1}{(T'(a)a)^2} = \frac{8\pi\rho}{3 + 8\pi l^2 \rho}, \quad (9)$$

$$\dot{H} + H^2 = \frac{4\pi\rho(-3 + 16\pi l^2 \rho)}{(3 + 8\pi l^2 \rho)^2}, \quad (10)$$

where $H = \frac{\dot{a}}{a}$ and the prime stands for the derivative with respect to a . Condition (8) is the consequence of the conservation of the energy-momentum tensor for dust, $\nabla_\mu \mathcal{T}^{\mu\nu} = 0$, where $\mathcal{T}^{\mu\nu} = \rho k^\mu k^\nu$ and $k^\mu \partial_\mu = \partial_T$. It is compatible with the two mentioned theories that identify the Hayward metric as

a vacuum solution [29, 39, 41]³. The corrected Friedmann equations given above reproduce the dynamical equations of a dust FRW cosmology in GR both in the low energy limit (at leading order when ρ is small) and in the limit $l \rightarrow 0$. Note also that, in the limit $a \rightarrow 0$, the energy density is clearly infinite. This issue will be discussed in Sec. IV.

We have numerically computed the scale factor, its first T -derivative, and the square Hubble parameter (for $M = 15$ and $a_0 = 5$ in Planck units). We display the results in Fig. 1. The most crucial step in this computation is inverting Eq. (7) to calculate $a(T)$. For this goal, we used libraries of JULIA programming language. This numerical calculation supports our statements in the previous paragraphs, concerning the smooth transition from de Sitter to power-law expansion, providing a graceful exit.

III. CONFORMAL DIAGRAM

In order to discuss the properties of the model, in particular in the context of the black hole information paradox, a useful tool is the conformal diagram of our spacetime. We have numerically generated the diagram in a rigorous manner that we comment in the following. This rigorous and unambiguous procedure is important to avoid confusions in the interpretation of the results, which are presented in Fig. 2.

We first adopt Painlevé-Gullstrand (PG) coordinates for the exterior. They simplify the construction, because the PG time and the time coordinate in Eq. (3) coincide⁴. Thus, we can write $dT = dt + (1/F)\sqrt{1-F}dX$, and metric (1) becomes

$$ds_{\text{ext}}^2 = -dT^2 + \left(dX + \sqrt{1-F(X)}dT \right)^2 + X^2 d\Omega. \quad (11)$$

Next, let's introduce double null coordinates

$$u = T - \int_0^X \frac{1}{1 - \sqrt{1-F}} d\tilde{X}, \quad (12)$$

$$v = T + \int_0^X \frac{1}{1 + \sqrt{1-F}} d\tilde{X}.$$

The integrand in the expression of $v(T, X)$ is regular, whereas the one for $u(T, X)$ is not. However, it can be handled with methods similar to those presented in Ref. [24] (see the discussion around Eqs.

³ The conservation law indeed holds for the four-dimensional variant of the theory with an infinite tower of higher-order corrections when the FRW ansatz is adopted (see the discussion around Eq. (7) in Ref. [41]).

⁴ This follows from the fact that the PG time coordinate is, by construction, the affine parameter of free-falling observers, exactly the same as the time coordinate used in Eq. (3).

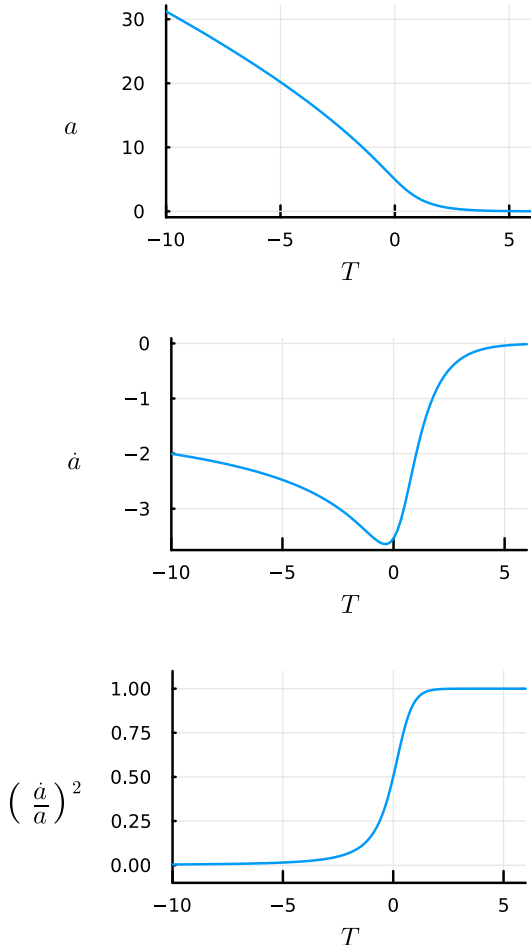


Figure 1. Time dependence of the scale factor, of its first time derivative, and of the square Hubble parameter (from top to bottom). The Universe follows a power-law contraction at early times and then smoothly transits to a de Sitter-like epoch at late times. We have taken $M = 15$ and $a_0 = 5$ (in Planck units).

2.29-3.31). These null coordinates still need to be appropriately compactified. The construction of the corresponding global coordinate system (\tilde{u}, \tilde{v}) (covering both the exterior and the interior) is performed in Appendix B.

The conformal diagram in Fig. 2 represents the collapse of a dust ball forming a Hayward black hole. The surface of the collapsing ball, at $r = r_b$, starts from $X \rightarrow \infty$ and crosses the pair of horizons X^+ and X^- , where $u \rightarrow \infty$ and $u \rightarrow -\infty$, respectively. Finally, it reaches $X = 0$, where $u \rightarrow \infty$ and $v \rightarrow \infty$, in an infinite affine time according to co-moving observers. This endpoint is also reached in the diagram by the horizon $X = X^-$. Similarly, the trajectory of the origin of the radial coordinate ($r = 0$) in the FRW interior also terminates there (see Appendix B for the demonstration). Interestingly, the only radial null geodesic that reaches that point, i.e. the final collapsing point, is also a $X = X^-$ horizon genera-

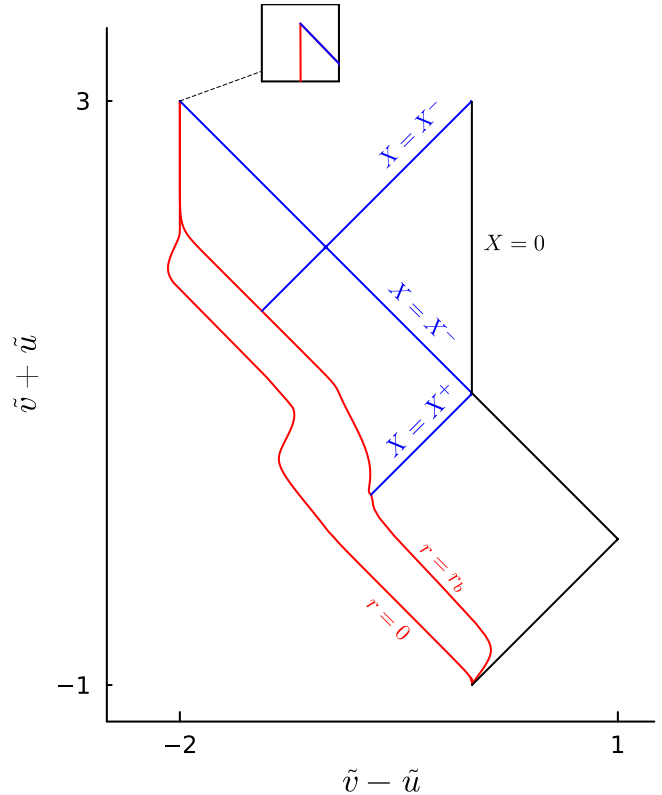


Figure 2. Conformal diagram representing our (quantum mechanically) modified OS collapse scenario. The FRW geometry, enclosed by curves marked by $r = 0$ and $r = r_b$, is surrounded by the static Hayward black hole geometry, with horizons $X = X_-$ and $X = X_+$. We have taken $M = 15$, $a_0 = 5$, $r_b = (4\pi/3)^{-1/3}$ and $\kappa = 0.1$ (in Planck units).

tor. The rest of radial null geodesics either leave the collapsing dust ball forever at some point or never enter it. We show in Appendix C that the geodesic in question reaches the final point in infinite affine time. The regular quantum gravity core, represented by the timelike line $X = 0$, is causally disconnected from the dust content. The diagram may be analytically extended beyond $X = X^-$ at the top to reproduce infinitely many copies of the Hayward static geometry there.

IV. DISCUSSION

In this work, starting with the Hayward black hole metric and imposing junction conditions on the surface of a collapsing dust ball, we have constructed the complete geometry of a modified OS collapse model, which includes corrections arising from Planck scales. The Hayward exterior is static, whereas the interior is described by a homogeneous cosmology for which we have deduced corrected Friedmann equations. The resulting spacetime is geodesically complete. A power-law contraction of

the interior dust matter precedes a smooth transition to a de Sitter phase. Although here the time orientation is chosen so that the model describes gravitational collapse, the cosmological evolution admits also a time-reversed version, in which de Sitter inflation is followed by a graceful exit to a power-law behavior. Qualitatively, this cosmological evolution resembles the one found in the Starobinsky model [47]. Moreover, cosmic inflation plays in the model an unexpected role, namely, it provides a (quantum) mechanism that decelerates the collapsing matter so that a Schwarzschild-like singularity is never formed.

The conformal diagram of our modified OS collapse model is shown in Fig. 2. This diagram provides the global causal structure of the model. Before computing the diagram, it was not obvious whether the collapsing matter might terminate at the crossing point of the X^- horizon and the core, $X = 0$. Remarkably, the whole congruence of r -constant time-like geodesics actually ends up there forming a caustic. However, the fact that such point is reached after an infinite amount of affine time of the free-falling observers may suggest that the associated divergence of the energy density $\rho \rightarrow \infty$ would be absent in a more realistic collapse scenario accounting for the back-reaction of the Hawking radiation. The diagram representing the evaporation of the Hayward black hole (see Fig. 5 in Ref. [5]) indicates that the black hole lifetime is finite for free-falling observers, so that, in our model, the whole black hole mass could evaporate before $T \rightarrow \infty$. Similarly, the only radial null geodesic reaching the final collapsing point arrives there in infinite affine time. Surprisingly, for an FRW dust cosmology governed by Eqs. (3) and (9), the geodesic completeness could be spoiled. That is, for a cosmological model beyond OS, i.e. $r \in [0, \infty)$, there might be infinitely radial null geodesics reaching $a \rightarrow 0$ in finite affine time. One may speculate that the cosmology studied here is geodesically complete only when surrounded by the static black hole metric. However, the analysis of the corresponding model without the black hole is beyond the scope of this work. Nevertheless, our model teaches us a lesson, namely, that inflationary cosmological spacetimes, where $r \in [0, r_b]$, might be past (or future) complete when the exterior vacua are described by smoothly joined black hole metrics. In this way, such models may circumvent the Borde-Guth-Vilenkin theorem [48], which states that spacetimes of this type are incomplete when $r \in [0, \infty)$.

Besides, the diagram indicates that the presence of the inner horizon may probably lead to instabilities, known in the literature as ‘mass inflation’ [49]. In particular, the main reason argued for the appearance of instabilities is that light rays traveling in the vicinity of the inner horizon would experience an arbitrarily high blueshift. However, the overall situation again might be cured by taking into con-

sideration the back-reaction of the Hawking quanta, as advocated by Hayward (since a black hole evaporates, an inner horizon is no more real than the event horizon [5]). Preliminary investigations supporting this possibility were recently conducted in Ref. [17]. Nonetheless, the construction of a conformal diagram that incorporates the consequences of Hawking radiation, at least effectively, is beyond the scope of this work. It would be interesting to see whether Fig. 5 in Ref. [5] is significantly modified when one considers the dust collapse presented here, instead of Vaidya-like ingoing energy flux forming the black hole.

Our model finds motivation in the recently proved fact that the Hayward metric is a vacuum solution of two different effective theories that incorporate quantum gravity corrections, namely, Quasi-Topological gravity [39, 41] and LQG-inspired LTB models [29]. Remarkably, the time dynamics of the scale factor which we have derived (see Fig. 1) are similar to the evolution displayed in Fig. 1 of Ref. [41] and in Fig. 5 of Ref. [29]. This further supports the compatibility of our OS collapse model with those effective approaches.

The considered model presents several clear advantages with respect to other alternatives discussed in the literature. In this sense, it is worth emphasizing the relative simplicity of the cosmological dynamics governed by Eq. (9), the non-singular nature of the resulting spacetime and, most importantly, the inflationary phase that may successfully describe early stages of our universe. In contrast, bouncing OS dust collapse models coming from standard LQG techniques [23–38] are singular, because they admit Reissner-Nordström-like singularities in vacuo⁵. On the other hand, going beyond OS to the case of inhomogeneous dust collapse, the standard LQG techniques lead to shell-crossing singularities [34]. On the contrary, the geometry of the model proposed in this work is smooth everywhere, unlike that in Refs. [38, 43]. Let us also point out that there exist similarities between the dynamics of the model and the quantum-inspired gravitational collapse considered in Ref. [7]. A Taylor expansion of the right-hand side of Eq. (9) around $\rho = 0$ yields an infinite tower of (quantum) corrections characterized by consecutive powers of ρ and l . These corrections were truncated at ρ^3 in Ref. [7] (see the discussion around Eq. (23) in that work). However, the cosmological interiors obtained in Ref. [7] may lead to timelike singularities in the exterior, just like in the case of standard LQG models, because the corresponding modified Friedmann equations are similar (see Eq.

⁵ Notice also that the careful analysis carried out in Refs. [27, 34] shows the singular behavior of the models proposed in Refs. [30–33] and of their causal structures.

(24) in Ref. [7] and Eq. (2) in Ref. [25]). The inhomogeneous variant [50] of Ref. [7] is also affected by comparable problems. Thus, we see that a fully detailed study of the causal structure is necessary to decide whether the spacetime is actually non-singular. Indeed, the analysis in this work shows the importance of a rigorous construction of the conformal diagram in collapse models. It would be interesting to see whether some crucial features (for example, singularities) of the models in Refs. [6–8, 10, 11, 14–16, 18–22] remain hidden because their conformal diagrams have not been obtained. Interestingly, our dust collapse model shows also a remarkable resemblance with the model obtained in Ref. [44] using ASG. More concretely, the scale factor and the exterior metric function behave qualitatively in the same way (see Figs. 1 and 2 in that reference), and the dust energy density also diverges. Thus, one can expect that the conformal diagram obtained here (but absent in Ref. [44]) and all the consequences derived from it would apply also to that case. However, our model does not require a running Newton gravitational “constant”, a phenomenon which has not been (at least so far) experimentally supported.

Summarizing, our model represents a clear advance, with important improvements compared to other proposals published in the literature inasmuch as it simultaneously displays the following good physical properties. (i) It does not need to introduce new degrees of freedom, or matter fields additional to those of the case of dust collapse in GR, or a running gravitational constant. (ii) It has a relatively simple cosmological dynamics that may successfully describe the early stages of our universe (with graceful exit from exponential inflation). (iii) The resulting spacetime is nonsingular (this fact was verified by a detailed analysis of the causal structure).

Finally, the modified Friedmann equations that we have obtained provide a possible route to analyse observational effects in cosmology. Especially, it would be interesting to study if they determine the dynamics of primordial perturbations, which would serve as seeds for the Cosmic Microwave Background (CMB).

ACKNOWLEDGEMENTS

The author would like to thank Tomasz Pawłowski and Guillermo A. Mena Marugán for discussions and help in the preparation of the manuscript. This work was supported in part by the Polish National Center for Science (Narodowe Centrum Nauki – NCN) grant OPUS 2020/37/B/ST2/03604.

Appendix A: the Kretschmann scalar for the interior

The Kretschmann scalar for the line element (3), with the scale factor a determined by the inverse of $T(a)$ given in Eq. (7), can be calculated to be

$$\begin{aligned} K_{\text{int}} &= \frac{12(a^2 T''(a)^2 + T'(a)^2)}{a^4 T'(a)^6} = \\ &= \frac{12M^2(5a^6 r_b^6 + 8a^3 l^2 M r_b^3 + 32l^4 M^2)}{(a^3 r_b^3 + 2l^2 M)^4}. \end{aligned} \quad (\text{A1})$$

Appendix B: Construction of the global coordinate system

To cover the exterior region in Fig. 2, we perform the compactification

$$\begin{aligned} \tilde{u} &= \pm \arctan(\kappa u)/\pi + c_u, \\ \tilde{v} &= \pm \arctan(\kappa v)/\pi + c_v, \end{aligned} \quad (\text{B1})$$

where $c_v \in \{0, 1\}$, $c_u \in \{0, 1, 2\}$, and κ are suitably chosen constants. For the sake of an example, consider the trajectory of the surface given by the pair $\{u(T, R(T)), v(T, R(T))\}$. The u coordinate reaches infinity exactly at $R \rightarrow X^+$. So, to obtain a monotonic and compactified coordinate \tilde{u} , we have to choose $c_u = 0$ and the plus sign in front of the arctan function for $R > X^+$, and correspondingly $c_u = 1$ and the minus sign for $X^- < R < X^+$. Similarly, the u coordinate reaches minus infinity exactly at $R \rightarrow X^-$. Thus, we choose $c_u = 2$ and the plus sign for $R < X^-$. The coordinate v is already monotonic for the trajectory of the surface, so we take $c_v = 0$ and the plus sign in this case. However, to cover the vacuum part enclosed by $X = X^-$ and $X = 0$ (see Fig. 2), we have to choose $c_v = 1$ and the minus sign. Of course, we have to appropriately match signs and constants whenever the surfaces X^- or X^+ are crossed. As for κ , it is simply a dimensionless, positive constant that allows us to adjust the form of the diagram. The above construction is a simplified (but equally general) version of the procedure presented in Ref. [51].

To extend Eq. (B1) to the interior, we follow the method developed in Ref. [46]. We define

$$u_{\text{int}} = \int_0^T \frac{1}{a(\tilde{T})} d\tilde{T} - r, \quad v_{\text{int}} = u_{\text{int}} + 2r, \quad (\text{B2})$$

as the double null coordinates for the interior line element (3). Then, the extension of (B1) is given by

$$\begin{aligned} \tilde{u}(T, r) &= \pm \arctan[\kappa u(T\{u_{\text{int}}(T, r)\})]/\pi + c_u, \\ \tilde{v}(T, r) &= \pm \arctan[\kappa v(T\{v_{\text{int}}(T, r)\})]/\pi + c_v, \end{aligned} \quad (\text{B3})$$

where $T\{u_{\text{int}}\}$ and $T\{v_{\text{int}}\}$ are, respectively, the inverse of $u_{\text{int}}(T, r = r_b)$ and $v_{\text{int}}(T, r = r_b)$. With the above coordinates, we can plot for instance the trajectory $(\tilde{u}(T, r = 0), \tilde{v}(T, r = 0))$, as displayed in Fig. 2. We point out that, in the limit $T \rightarrow \infty$, the whole r -constant congruence of timelike geodesics, with $0 \leq r \leq r_b$, terminate at the same point of the conformal diagram. Since the scale factor a goes to zero in this limit, the integral in Eq. (B2) then diverges. In other words, for all the geodesics $0 \leq r \leq r_b$, we have

$$\lim_{T \rightarrow \infty} u_{\text{int}} = 0, \quad \lim_{T \rightarrow \infty} v_{\text{int}} = \infty.$$

Therefore, the values of the double null coordinates (B2), or alternatively (B3), coincide in all the congruence at $T \rightarrow \infty$. One can also check this statement by explicitly computing the integral via a change of variables $a = a(T)$ and utilizing Eq. (7).

We refer to Ref. [46] for the detailed construction and limitations of the presented method.

Appendix C: Unique radial null geodesic reaching the final collapsing point

We will now show that the radial null geodesic which is also a $X = X^-$ horizon generator (see Fig.

2) takes an infinite affine time to reach the final collapsing point. We rewrite the metric (1) using outgoing Eddington-Finkelstein (EF) coordinates defined by a condition coming from (12), namely $du = dt - dX/F(X)$. This leads to

$$ds_{\text{ext}}^2 = -F(X)du^2 - 2dudX + X^2d\Omega^2. \quad (\text{C1})$$

Let the coordinate u be a parameter of a family of radial null geodesics, so that the tangent vector in EF coordinates is given by $q^\alpha = (1, -F(X)/2)$. We have for the four-acceleration $q^\alpha \nabla_\alpha q^\beta = -(dF/dX)q^\beta/2$. Let λ^* be the affine parameter. The parameters are related by the differential equation (see Chapter 1.3 of [45] for a general discussion)

$$\frac{d^2\lambda^*}{du^2} = -\frac{1}{2} \frac{dF}{dX} \frac{d\lambda^*}{du}. \quad (\text{C2})$$

The solution is

$$\lambda^*(u) = -2c_1 \left(\frac{dF}{dX} \right)^{-1} \exp \left(-\frac{1}{2} \frac{dF}{dX} u \right) + c_2, \quad (\text{C3})$$

where c_1 and c_2 are integration constants. For the $X = X^-$ horizon generator, we have $dF/dX = \text{const.} < 0$. Thus, when the final collapsing point is reached, with $u \rightarrow \infty$, the affine parameter λ^* diverges.

-
- [1] J. R. Oppenheimer and H. Snyder, *Phys. Rev.* **56**, 455 (1939).
 - [2] A. Ashtekar and M. Bojowald, *Class. Quant. Grav.* **22**, 3349 (2005), arXiv:gr-qc/0504029.
 - [3] E. Poisson and W. Israel, *Class. Quant. Grav.* **5**, L201 (1988).
 - [4] I. Dymnikova, *Gen. Rel. Grav.* **24**, 235 (1992).
 - [5] S. A. Hayward, *Phys. Rev. Lett.* **96**, 031103 (2006), arXiv:gr-qc/0506126.
 - [6] C. Barragan, G. J. Olmo, and H. Sanchis-Alepuz, *Phys. Rev. D* **80**, 024016 (2009), arXiv:0907.0318 [gr-qc].
 - [7] C. Bambi, D. Malafarina, and L. Modesto, *Phys. Rev. D* **88**, 044009 (2013), arXiv:1305.4790 [gr-qc].
 - [8] A. Saini and D. Stojkovic, *Phys. Rev. D* **89**, 044003 (2014), arXiv:1401.6182 [gr-qc].
 - [9] T. De Lorenzo, C. Pacilio, C. Rovelli, and S. Speziale, *Gen. Rel. Grav.* **47**, 41 (2015), arXiv:1412.6015 [gr-qc].
 - [10] V. P. Frolov, *Phys. Rev. Lett.* **115**, 051102 (2015), arXiv:1505.00492 [hep-th].
 - [11] V. P. Frolov, A. Zelnikov, and T. de Paula Netto, *JHEP* **06**, 107 (2015), arXiv:1504.00412 [hep-th].
 - [12] V. P. Frolov, *Phys. Rev. D* **94**, 104056 (2016), arXiv:1609.01758 [gr-qc].
 - [13] R. Carballo-Rubio, F. Di Filippo, S. Liberati, C. Pacilio, and M. Visser, *JHEP* **07**, 023 (2018), arXiv:1805.02675 [gr-qc].
 - [14] C. Kiefer and T. Schmitz, *Phys. Rev. D* **99**, 126010 (2019), arXiv:1904.13220 [gr-qc].
 - [15] K. Mosani, K. Mosani, D. Dey, D. Dey, P. S. Joshi, and P. S. Joshi, *Phys. Rev. D* **101**, 044052 (2020), [Erratum: *Phys.Rev.D* **107**, 069903 (2023)], arXiv:2001.04367 [gr-qc].
 - [16] A. Gózdź, M. Kisielowski, and W. Piechocki, *Phys. Rev. D* **107**, 046019 (2023), arXiv:2211.05401 [gr-qc].
 - [17] A. Bonanno, A.-P. Khosravi, and F. Saueressig, *Phys. Rev. D* **107**, 024005 (2023), arXiv:2209.10612 [gr-qc].
 - [18] M. Shafiee and Y. Bahrampour, *JHEP* **06**, 055 (2023), arXiv:2212.00466 [hep-th].
 - [19] C. Kiefer and H. Mohaddes, *Phys. Rev. D* **107**, 126006 (2023), arXiv:2303.17924 [gr-qc].
 - [20] A. Alonso-Bardaji and D. Brizuela, *Phys. Rev. D* **109**, 064023 (2024), arXiv:2312.15505 [gr-qc].
 - [21] E. I. Duque, *Phys. Rev. D* **109**, 044014 (2024), arXiv:2311.08616 [gr-qc].
 - [22] G. Barca and G. Montani, *Eur. Phys. J. C* **84**, 261 (2024), arXiv:2309.09767 [gr-qc].
 - [23] M. Bobula, 'Radiation in quantum gravitational collapse,' <https://indico.cern.ch/event/1100970/>, LOOPS'22 (18-22 July 2022), ENS de Lyon.
 - [24] M. Bobula and T. Pawłowski, *Phys. Rev. D* **108**, 026016 (2023), arXiv:2303.12708 [gr-qc].
 - [25] J. Lewandowski, Y. Ma, J. Yang, and C. Zhang, *Phys. Rev. Lett.* **130**, 101501 (2023), arXiv:2210.02253 [gr-qc].
 - [26] K. Giesel, M. Han, B.-F. Li, H. Liu, and P. Singh, *Phys. Rev. D* **107**, 044047 (2023), arXiv:2212.01930

- [gr-qc].
- [27] K. Giesel, H. Liu, P. Singh, and S. A. Weigl, (2023), arXiv:2308.10953 [gr-qc].
- [28] K. Giesel, H. Liu, E. Rullit, P. Singh, and S. A. Weigl, (2023), arXiv:2308.10949 [gr-qc].
- [29] K. Giesel, H. Liu, P. Singh, and S. A. Weigl, (2024), arXiv:2405.03554 [gr-qc].
- [30] J. G. Kelly, R. Santacruz, and E. Wilson-Ewing, *Class. Quant. Grav.* **38**, 04LT01 (2021), arXiv:2006.09325 [gr-qc].
- [31] J. G. Kelly, R. Santacruz, and E. Wilson-Ewing, *Phys. Rev. D* **102**, 106024 (2020), arXiv:2006.09302 [gr-qc].
- [32] V. Husain, J. G. Kelly, R. Santacruz, and E. Wilson-Ewing, *Phys. Rev. Lett.* **128**, 121301 (2022), arXiv:2109.08667 [gr-qc].
- [33] V. Husain, J. G. Kelly, R. Santacruz, and E. Wilson-Ewing, *Phys. Rev. D* **106**, 024014 (2022), arXiv:2203.04238 [gr-qc].
- [34] F. Fazzini, V. Husain, and E. Wilson-Ewing, *Phys. Rev. D* **109**, 084052 (2024), arXiv:2312.02032 [gr-qc].
- [35] F. Fazzini, C. Rovelli, and F. Soltani, *Phys. Rev. D* **108**, 044009 (2023), arXiv:2307.07797 [gr-qc].
- [36] L. Cafaro and J. Lewandowski, (2024), arXiv:2403.01910 [gr-qc].
- [37] L. Cipriani, F. Fazzini, and E. Wilson-Ewing, (2024), arXiv:2404.04192 [gr-qc].
- [38] M. Han, D. Qu, and C. Zhang, (2024), arXiv:2404.02796 [gr-qc].
- [39] P. Bueno, P. A. Cano, and R. A. Hennigar, (2024), arXiv:2403.04827 [gr-qc].
- [40] S. E. Aguilar-Gutierrez, P. Bueno, P. A. Cano, R. A. Hennigar, and Q. Llorens, *Phys. Rev. D* **108**, 124075 (2023), arXiv:2310.09333 [hep-th].
- [41] G. Arciniega, P. Bueno, P. A. Cano, J. D. Edelstein, R. A. Hennigar, and L. G. Jaime, *Phys. Lett. B* **802**, 135242 (2020), arXiv:1812.11187 [hep-th].
- [42] P. Bueno, P. A. Cano, and R. A. Hennigar, *Phys. Rev. Lett.* **132**, 191402 (2024), arXiv:2312.04637 [hep-th].
- [43] M. Han, C. Rovelli, and F. Soltani, *Phys. Rev. D* **107**, 064011 (2023), arXiv:2302.03872 [gr-qc].
- [44] A. Bonanno, D. Malafarina, and A. Panassiti, *Phys. Rev. Lett.* **132**, 031401 (2024), arXiv:2308.10890 [gr-qc].
- [45] E. Poisson, *A Relativist's Toolkit: The Mathematics of Black-Hole Mechanics* (Cambridge University Press, 2009).
- [46] M. Bobula and T. Pawłowski, (2024).
- [47] A. A. Starobinsky, *Phys. Lett. B* **91**, 99 (1980).
- [48] A. Borde, A. H. Guth, and A. Vilenkin, *Phys. Rev. Lett.* **90**, 151301 (2003), arXiv:gr-qc/0110012.
- [49] E. Poisson and W. Israel, *Phys. Rev. Lett.* **63**, 1663 (1989).
- [50] Y. Liu, D. Malafarina, L. Modesto, and C. Bambi, *Phys. Rev. D* **90**, 044040 (2014), arXiv:1405.7249 [gr-qc].
- [51] J. C. Schindler and A. Aguirre, *Class. Quant. Grav.* **35**, 105019 (2018), arXiv:1802.02263 [gr-qc].